1981A&A...102..207D

Astron. Astrophys. 102, 207–211 (1981)

ASTRONOMY AND ASTROPHYSICS

Analysis of the Far Ultraviolet Emission Lines in Late Type Stars*

E. de Castro[1], M.J. Fernández-Figueroa[1], M. Rego[1], and D. Ponz[2]

[1] Departamento de Astrofísica, Facultad de Físicas, Universidad Complutense, Ciudad Universitaria, Madrid-3, Spain
[2] Villafranca Satellite Tracking Station Apartado 54065, Madrid, Spain

Received December 15, 1980; accepted March 27, 1981

Summary. Far ultraviolet emission lines in a sample of seven stars of spectral type later than F5 and different luminosity class have been analyzed to calculate the electron density and pressure in the formation region of the lines. Three different methods were used. We obtain electron pressures larger than solar for all dwarf stars of the sample. The low resolution observations were made with the IUE satellite.

Key words: emission lines – transition region – corona

1. Introduction

The main source of information about the outer stellar regions of intermediate and late type stars are far ultraviolet observations. The emission lines in this spectral region are associated with chromospheres, transition regions and coronae.

Until quite recently most of our knowledge of outer stellar regions has come from studying the Ca II H and K emission lines in late type stars. Later the Mg II h and k and the He I λ 10830 Å lines were added as indicators of chromospheres, transition regions and coronae.

The IUE satellite now provides a valuable opportunity to study the ultraviolet spectra of cool stars in more detail, and allows to improve the information about the structure of these outer regions.

The presence of emission lines in the spectral range λ 1100–2000 Å indicates a plasma with temperatures larger than 10,000 K. For late type stars one distinguishes between two groups, one with a solar type transition region as well as corona and another with no indication of material hotter than 20,000 K (Linsky and Haisch, 1979). The dwarf stars of this work must be included in the first group.

In this paper we analyze the ultraviolet emission lines in a sample of stars of spectral type later than F5.

2. Observations

A sample of seven stars of different temperatures and luminosity class showing Ca II H and K emission lines has been chosen. The effective temperature of the atmosphere has been derived from the broad-band color of Johnson et al. (1966) using the mean color-$T_{\rm eff}$ relations of Johnson (1966). The Ca II K intensity (Wilson and Bappu, 1957), the full width at the base (FWB) of Mg II k (Rego et al., 1979; Weiler and Oegerle, 1979) and the equivalent width of He I λ10,830 Å (Zirin, 1976) are given in Tables 1 and 2.

Table 1. Stellar parameters

HD	Name	Sp.T.	m_v	$B-V$	$V-I$	$V-R$	$T_{\rm eff}$
3712	αCas	K0II–III	2.2	1.17	1.38	0.78	4550
4502	ζAnd	K1III	4.1	1.10	1.44	0.85	4500
20630	κCet	G5V	4.8	0.68	0.93	0.57	5600
62509	βGem	K0III	1.1	1.00	1.25	0.75	4800
114710	βCom	G0V	4.3	0.58	0.79	0.49	5900
124850	iVir	F7IV	4.1	0.51	0.77	0.50	6200
142373	χHer	F9V	4.6	0.57	0.80	0.48	6000

Table 2. Chromospheric indicators

HD	I (K CaII)	FWB (k MgII)	W (He)
3712	2	—	0
4502	5	187 km/s [a]	760 mÅ
20630	3	128 km/s [b]	200 mÅ
62509	2	193 km/s [a]	140 mÅ
114710	1	124 km/s [b]	—
124850	1	—	—
142373	1	—	—

[a] Weiler and Oegerle (1979) [b] Rego et al. (1979)

Table 3. Observational data

HD	t (min)	Image no.
3712	150	SWP 6697
4502	50	SWP 6834
20630	50	SWP 9462
62509	20	SWP 6472
114710	63	SWP 9465
124850	60	SWP 9464
142373	80	SWP 9463

Send offprint requests to: M.J. Fernández-Figueroa

* Based on observations by the International Ultraviolet Explorer collected at the Villafranca Satellite Tracking Station of the European Space Agency

© European Southern Observatory • Provided by the NASA Astrophysics Data System

1981A&A...102..207D

IUE low resolution (≃6 Å) observations were obtained in the spectral range λλ1150–2000 Å with the SWP camera. The exposure time and the image number for each star are given in Table 3. Three stars of the sample αCas, ζAnd, and βGem were not observed by us, but their images were released to the scientific community in June 1980.

Several emission lines of C, O, N, Si in different ionization states have been identified in all spectra. The identified lines, the observed fluxes and the surface fluxes, both in erg cm^{-2} s^{-1}, are listed in Tables 4a and 4b for each star. Observed line fluxes have been transformed into surface fluxes with the angular diameter obtained by the relations of Barnes and Evans (1976) as well as Barnes et al. (1976). For αCass it was necessary to correct for interstellar extinction by means of the ultraviolet interstellar extinction law $\log F_\lambda^{cor} = \log F_\lambda^{ob} + 0.43\, k_\lambda\, E(B-V)$, where k_λ is the total extinction per unit visual color excess, $E(B-V)$, obtained by Nandy (1976) and Seaton (1979).

The normal short wavelength limit of the IUE SWP spectra is λ1150 Å, however this limit was effectively moved up to about λ1230 Å in our observations. The long exposure time required makes the geocoronal Lyα quite strong, disturbing any feature between λ1200 and λ1230 Å. On the other hand, the long wavelength limit is approximately λ1830 Å for the hotter stars of the sample due to the absorption edge of Si I.

An upper limit of 3σ has been included in the fluxes listed in Table 4 when the line was not observed.

Table 4a and b. Observed and surface fluxes both in erg cm^{-2} s^{-1}

Table 4a

λ (Å)	El	HD 20630		HD 114710		HD 124850		HD 142373	
		F_{ob}	F_*	F_{ob}	F_*	F_{ob}	F_*	F_{ob}	F_*
1240	N V	6.22 (−14)	9.81 (3)	6.23 (−14)	8.13 (3)	6.19 (−14)	6.06 (3)	5.42 (−14)	9.09 (3)
1304	O I	7.06 (−14)	1.11 (4)	2.34 (−14)	3.05 (3)	1.60 (−13)	1.56 (4)	5.44 (−14)	9.12 (3)
1335	C II	1.37 (−13)	2.17 (4)	3.25 (−14)	4.23 (3)	2.42 (−13)	2.63 (4)	4.21 (−14)	7.06 (3)
1357	O I	2.72 (−13)	4.30 (4)	1.79 (−14)	2.34 (3)	7.95 (−14)	7.77 (3)	4.10 (−14)	6.88 (3)
1394	Si IV	7.66 (−14)	1.21 (4)	2.37 (−14)	3.09 (3)	1.27 (−13)	1.24 (4)	4.45 (−14)	7.47 (3)
1403	Si IV	7.04 (−14)	1.11 (4)	2.96 (−14)	3.86 (3)	9.81 (−14)	9.60 (3)	4.09 (−14)	6.83 (3)
1482	S I	5.96 (−14)	9.41 (3)	3.66 (−14)	4.79 (3)	1.09 (−13)	1.06 (4)	8.33 (−14)	1.39 (4)
1530	Si II	6.65 (−14)	1.99 (4)	7.28 (−14)	9.50 (3)	3.03 (−13)	2.96 (4)	8.99 (−14)	1.51 (4)
1550	C IV	2.17 (−13)	2.47 (4)	7.14 (−14)	9.32 (3)	3.43 (−13)	3.36 (4)	9.39 (−14)	1.58 (4)
1640	He II	6.00 (−14)	9.47 (3)	3.06 (−14)	4.00 (3)	2.76 (−13)	2.70 (4)	—	—
1657	C I	1.47 (−13)	2.31 (4)	8.07 (−14)	1.05 (4)	1.90 (−13)	2.84 (4)	9.94 (−14)	1.67 (4)
1748	Ni II	1.33 (−13)	2.10 (4)	—	—	—	—	—	—
1808	Si II	2.19 (−13)	3.45 (4)	1.65 (−13)	2.15 (4)	sat	sat	<3.36 (−13)	<5.63 (4)
1817	Si II	2.87 (−13)	4.53 (4)	1.92 (−13)	2.51 (4)	sat	sat	<4.35 (−13)	<7.31 (4)
1892	Si III	2.52 (−13)	3.97 (4)	<3.37 (−13)	<4.04 (4)	sat	sat	sat	sat
1909	C III	3.02 (−13)	4.77 (4)	<3.67 (−13)	<4.35 (4)	sat	sat	sat	sat

Table 4b

λ (Å)	El	HD 3712		HD 4502		HD 62509	
		F_{ob}	F_*	F_{ob}	F_*	F_{ob}	F_*
1240	N V	2.08 (−13)	9.04 (2)	2.49 (−13)	9.31 (3)	1.78 (−13)	4.50 (2)
1304	O I	1.09 (−12)	4.73 (3)	9.74 (−13)	3.62 (4)	5.52 (−13)	1.46 (3)
1335	C II	—	—	3.74 (−13)	1.16 (4)	1.80 (−13)	1.46 (3)
1357	O I	—	—	9.55 (−14)	3.58 (3)	—	—
1394	Si IV	1.14 (−14)	4.99 (2)	2.50 (−13)	8.40 (3)	1.08 (−13)	3.19 (2)
1403	Si IV	2.43 (−13)	1.05 (3)	1.98 (−13)	7.38 (3)	1.04 (−13)	2.76 (2)
1530	Si II	3.20 (−13)	1.34 (3)	1.11 (−13)	4.14 (3)	—	—
1550	C IV	<2.29 (−13)	<1.00 (3)	5.51 (−13)	2.06 (4)	2.03 (−13)	5.34 (2)
1640	He II	—	—	2.38 (−13)	8.88 (3)	1.74 (−13)	4.42 (2)
1657	C I	2.26 (−13)	9.86 (2)	2.37 (−13)	8.86 (3)	2.95 (−13)	7.71 (2)
1748	Ni II	—	—	1.13 (−13)	4.22 (3)	—	—
1808	Si II	<2.50 (−13)	<1.32 (3)	2.79 (−13)	1.04 (4)	3.89 (−13)	1.03 (3)
1817	Si II	<4.72 (−13)	<2.05 (3)	6.12 (−13)	2.28 (4)	5.27 (−13)	1.38 (3)
1892	Si III	<3.13 (−13)	<1.36 (3)	2.67 (−13)	9.96 (3)	<4.04 (−13)	<1.06 (3)
1909	C III	<3.30 (−13)	<1.43 (3)	1.90 (−13)	7.11 (3)	<3.60 (−13)	<9.41 (2)

© European Southern Observatory • Provided by the NASA Astrophysics Data System

1981A&A...102..207D

3. Results and Discussion

The ultraviolet spectra of all dwarf stars, namely κCet, βCom, and χHer, and of the subgiant iVir appear clearly similar to that of the quiet sun with typical lines of the solar transition region and corona. The more luminous stars βGem, ζAnd, and αCas show different spectra than the solar one, however it would not be correct to include these three stars into a single group, as for instance, high-temperature ions like C IV are present in βGem but not in αCass. On the other hand, the ultraviolet spectrum of the most luminous star, ζAnd, has similar lines and comparable surface fluxes to that found in solar active regions, this result is not surprising since ζAnd is a RS CVn star.

Figure 1 shows the H–R diagram with boundaries for circumstellar lines (Reimers, 1977), Mullan's (1978) supersonic transition locus, and the sharp empirical line of Linsky and Haisch (1979). We have located our stars on this diagram. Dwarf stars, the giant βGem and the subgiant iVir are shown to the left of all boundary lines, they are "solar type stars", while ζAnd is inmediately to the right of the Linsky and Haisch dividing line, although this line may not be as clearly defined as it appears in the figure (Linsky and Haisch, 1979). With respect to αCas, lies above all the boundaries and its spectrum shows rather weak emission lines and is very similar to spectra of "non solar type" stars. For this reason, αCas may be included in the supersonic wind class while the rest of the stars in our sample can be included in the transonic wind or coronal wind class.

The ratio of the C IV, Si IV and N V surface fluxes to the total surface flux are plotted versus $(B-V)$ in Fig. 2. All dwarf stars are more active than the sun and, apparently, there is no dependence on the effective temperature.

The number of more luminous stars is not enough to infer a dependence on the surface gravity, however the selected sample shows a similar scatter than that found by Linsky et al. (1978) from the Ca II line fluxes.

By assuming that the emission lines in the transition region and corona are optically thin and formed by collisional excitation from the ground state, the peak formation temperatures $T_{\max}$ for each line have been calculated, where $T_{\max}$ is the temperature at which the function $g(T)$ is a maximum,

$$g(T) = T_e^{-1/2}\, 10^{-5040W/T_e} \frac{N(\text{ion})}{N(\text{el})}.$$

T_e refers to electron temperature, W is the excitation potential, and $N(\text{ion})/N(\text{el})$ tabulated by Jordan (1969). According to these values the emission lines can be divided into three groups,

a)	$T < 2\,10^4$ K	C I, O I lines
b)	$2\,10^4 < T < 7\,10^4$ K	C II, Si II lines
c)	$T > 7\,10^4$ K	N V, C IV, Si IV lines

In all stars of our sample there are lines corresponding to each of these groups. The lines within group c are indicators of transition regions and possibly coronae, unfortunately the geocoronal Lyα line masks the identification of O V and O VI lines the formation temperature of which is about 10^6 K and could be proof of the existence of a corona.

The electron density in the region where ultraviolet emission lines are formed, has been calculated using three different methods.

1. Relative Intensities of Intercombination Lines

According to Doschek et al. (1978), the slope of the emission measure, $A_{\text{el}} N_e^2 V$, plotted as a function of temperature is the same in all stars. The line ratios C IV/Si IV and N V/Si IV are given in Fig. 3, for all stars in our sample and for stars included in the works of Linsky et al. (1978) and Jordan (1980). It is clear from the Fig. 3 that the conclusion of Doschek et al. (1978) is only valid for stars with the same luminosity class, this can be explained by the fact that the line ratio depends on density through the quantity $N(\text{ion})/N(\text{el})$ which is not the same for stars with different luminosity class.

If we assume the approximation proposed by Doschek et al. (1978), for electron densities lower than $10^{11}\,\text{cm}^{-3}$, the line ratio C III (λ1909)/Si III (λ1892) is proportional to N_e^{-1}. Using the

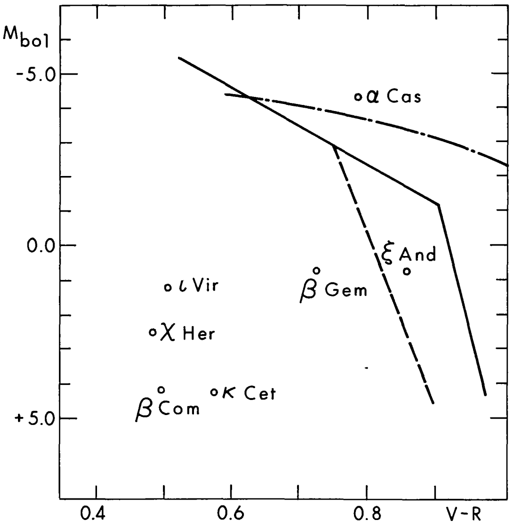

Fig. 1. H–R diagram for stars of our sample. The solid line is Mullan's, the dashed is from Haisch and Linsky and the dot-dashed is from Reimers

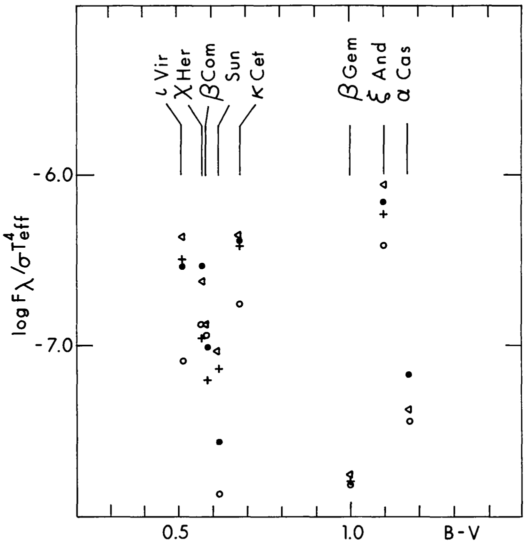

Fig. 2. Ratio surface flux to the total surface luminosity versus $(B-V)$, for C II λ1335 Å line (+), C IV λ1550 Å (Δ), Si IV λ1403 Å (●) and N V λ1240 Å (○)

© European Southern Observatory • Provided by the NASA Astrophysics Data System

1981A&A...102..207D

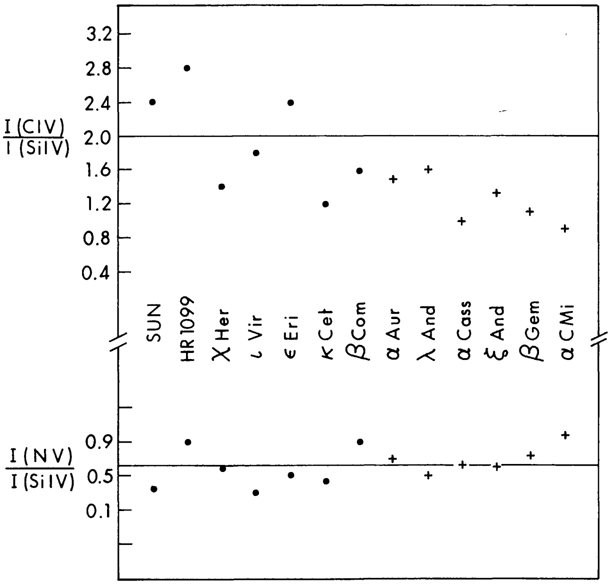

Fig. 3. Flux ratios of C IV (1550) and N V (1240) relative to Si IV (1403 + 1394) for the stars indicated. Filled points: luminosity class V, crosses: other luminosity classes

theoretical values deduced for the sun and the observed ratio for κCet we find an electron pressure $P_e = 8.32\,10^{14}\,\mathrm{cm}^{-3}\,\mathrm{K}$.

A similar method has been proposed by Cook and Nicolas (1979) using the lines λ1402 Si IV and λ1909 C III from which we obtain $P_e = 9\,10^{14}\,\mathrm{cm}^{-3}\,\mathrm{K}$.

In our sample the only star with C III and Si III lines and solar luminosity class is κCet, for this reason the method is only applied to this star.

2. *Energy Balance in the Transition Region*

Assuming the steady-state local energy equation in which the divergence of the downward conductive flux is balanced by radiative losses and the the collisional excitations are exactly balanced by radiative de-excitations, the surface flux ratios in the vicinity of T_{max} for each ion are given by,

$$\frac{F(*)}{F(\odot)} = \frac{A(\mathrm{el})_*}{A(\mathrm{el})_\odot}\,\frac{P_*}{P_\odot}$$

where A is the element abundance (Haisch and Linsky, 1976). The above relationship has been used to calculate the pressures listed in Table 5 for lines with peak temperature larger than 2×10^4 K. In all dwarf stars, the calculated pressure is larger than solar. Assuming $P_\odot = 0.15\,\mathrm{dyn\,cm}^{-2}$ we obtain $P_e = 10^{16}\,\mathrm{cm}^{-3}\,\mathrm{K}$ for κCet, that is 10^2 times larger than the value obtained previously.

3. *Cool Corona*

Several authors have suggested the existence of coronae with temperature lower than 10^6 K. Coronal line fluxes can be determined assuming that the line formation takes place in a plane – parallel isothermal region and are given by the relationship (McClintock et al., 1975),

$$F(\lambda) = \frac{7.07\,10^{25}\,\Omega}{g_1 \lambda T_c^{3/2}} A(\mathrm{el}) \frac{N(\mathrm{ion})}{N(\mathrm{el})} \exp(-W/kT_c) \frac{P^2}{g}$$

Table 5. Pressures obtained from the "energy balance" method

	$P_*/P_\odot$			
	1240	1335	1394	1550
HD 3712	1.5	—	0.9	0.2
HD 4502	17.3	4.0	7.8	5.6
HD 20630	9.6	4.0	6.2	5.0
HD 62509	0.3	0.1	0.1	0.1
HD 114710	5.0	0.5	4.8	0.6
HD 124850	19.0	1.8	18.0	4.0
HD 142373	19.0	4.0	17.0	6.0

Table 6. Total pressures obtained from the "cool corona" method

	$P_{\min(\text{cool corona})}$ dyn/cm^2
HD 3712	1.47 (−3)
HD 4502	2.2 (−3)
HD 20630	4.7 (−2)
HD 62509	1.0 (−3)
HD 114710	3.3 (−2)
HD 124850	2.5 (−2)
HD 142373	3.8 (−2)

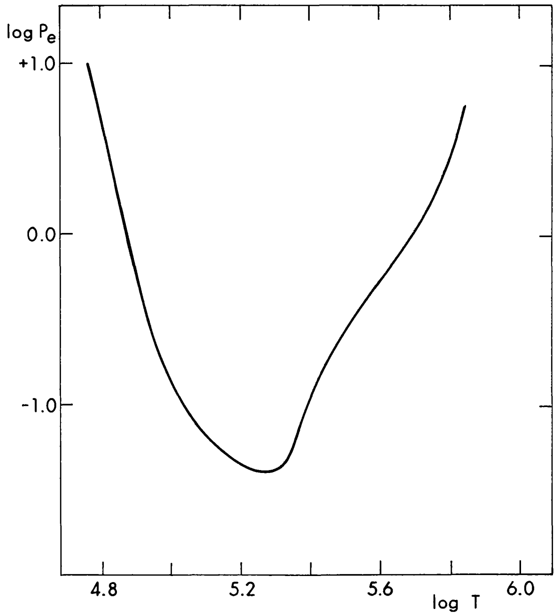

Fig. 4. Pressure as a function of temperature for N V 1240 Å line of κCet

where Ω is the collision cross-section, g_1 the statistical weight and g the surface gravity. In Fig. 4 the pressure, P, of κCet has been plotted as a function of temperature for N V 1240 Å. This curve shows the possible values of pressure for a corona of this type, the

© European Southern Observatory • Provided by the NASA Astrophysics Data System

1981A&A...102..207D

minimum value corresponding to T_{max}. The method provides a lower limit for the transition region pressure. Table 6 gives this lower limit for all the stars in our sample.

Errors in the computation of electron pressures using the above three methods are due to the uncertainty of the observed fluxes and are less than 20%. Errors due to uncertainties in atomic data or to the assumed hypotheses are not considered. The validity of our hypotheses are discussed in the conclusions.

4. Conclusions

All the stars in our sample show transition region and corona indicators similar to the sun except for αCas. The analyzed dwarf stars are more active than the sun.

For all observed dwarf stars the electron pressures obtained by each of three methods used are greater than the corresponding solar values.

The pressure of the giant βGem is lower than the dwarf stars. This suggests a trend of decreasing pressure with increasing stellar luminosity.

The line surface fluxes in ζAnd are higher by a factor of $\geqq 10$ than in the sun and the calculated pressures are similar to a solar active region. This result is not opposed to the above suggestion since ζAnd is a RS CVn star.

Our calculations are only approximate and the following limitations of the methods used should be noted,

The "relative intensities of intercombinations lines" method is only valid for solar luminosity class stars.

The "energy balance" method only defines an upper limit for the pressure and we have neglected the acoustic and magnetic fluxes which should perhaps be included.

From the "cool corona" method we have obtained a lower limit to the pressure in the transition region but, again, neglecting the acoustic and magnetic pressures.

These limits on electron pressure will be used as starting point in the development of a more elaborate model of the transition region.

References

Barnes, J.G., Evans, D.S.: 1976, *Monthly Notices Roy. Astron. Soc.* **174,** 489

Barnes, J.G., Evans, D.S., Parsons, S.B.: 1976, *Monthly Notices Roy. Astron. Soc.* **174,** 503

Brown, A., Jordan, C.: 1980, Proceedings of the Second European IUE Conference. Tübingen, Germany

Cook, J.W., Nicolas, K.R.: 1979, *Astrophys. J.* **229,** 1163

Doschek, G.A., Feldman, U., Mariska, J.T.: 1978, *Astrophys. J. Letters* **226,** L35

Haisch, B.M., Linsky, J.L.: 1976, *Astrophys. J. Letters* **205,** L39

Johnson, H.L.: 1966, *Ann. Rev. Astron. Astrophys.* **4,** 193

Johnson, H.L., Mitchell, R.I., Iriarte, B, Wisniewski, W.Z.: 1966, *Comm. Lunar Planetary Lab.* **4,** 99

Jordan, C.: 1969, *Monthly Notices Roy. Astron. Soc.* **142,** 501

Kelch, W.J., Linsky, J.L., Wordn, S.P.: 1979, *Astrophys. J.* **229,** 700

Linsky, J.L., Haisch, B.M.: 1979, *Astrophys. J. Letters* **229,** L27

Linsky, J.L., Wordn, S.P., McClintock, W., Robertson, R.M.: 1979, *Astrophys. J. Suppl.* **41,** 47

Linsky, J.L., Ayres, T.R., Basri, G.S., Morrison, N.D., Boggess, A., Schiffer III, F.H., Holm, A., Cassatella, A., Heck, A., Macchetto, F., Stickland, D., Wilson, R., Blanco, C., Dupree, A.K., Jordan, C., Wing, R.F.: 1978, *Nature* **275,** 389

McClintock, W., Linsky, J.L., Henry, R.C., Moos, H.W., Gerola, H.: 1975, *Astrophys. J.* **202,** 165

Mullan, D.J.: 1978, *Astrophys. J.* **226,** 51

Nandy, K., Thompson, G.I., Jamar, C., Monfils, A., Wilson, R.: 1976, *Astron. Astrophys.* **51,** 63

Pottasch, S.R.: 1964, *Space Sci. Rev.* **3,** 816

Rego, M., Fernández-Figueroa, M.J.: 1979, *Astron. Astrophys.* **76,** 249

Reimers, D.: 1977, *Astron. Astrophys.* **57,** 395

Seaton, M.J.: 1979, *Monthly Notices Roy. Astron. Soc.* **187,** 73

Seaton, M.J.: 1962, Atomic and molecular processes. Academic Press. New York

Weiler, E.J., Oegerle, W.R.: 1979, *Astrophys. J. Suppl.* **39,** 537

Wilson, O.C., Bappu, M.K.V.: 1957, *Astrophys. J.* **125,** 661

Zirin, H.: 1976, *Astrophys. J.* **208,** 414

© European Southern Observatory • Provided by the NASA Astrophysics Data System